

Green fabrication of iron oxide nanoparticles from *Lantana camara* leaf extract for degradation of methylene blue dye

K. Gilbert Ross Rex^{1*}, V. Akshaya¹, S. Santhiya¹, P. Bhuvaneshwari² and M. Rajamehala¹

¹Department of Biotechnology, Vivekanandha College of Engineering for Women, Namakkal-637 205, India

²Department of Biotechnology, Bharathidasan University, Trichy-620 024, India

Received: 30 October 2024

Revised: 08 February 2025

Accepted: 28 May 2025

*Corresponding Author Email: gilbertrossrex@gmail.com

*ORCID: <https://orcid.org/0000-0002-1364-3254>

Abstract

Aim: This study explores the green synthesis of iron oxide nanoparticles from the leaf extract of *Lantana camara* in order to test their efficacy for degradation of methylene blue dye.

Methodology: *Lantana camara* leaves were collected, washed, dried, crushed to fine powder, and dissolved in different amounts (1g, 5g, 10g and 15g) in distilled water. For nanoparticle synthesis, ferric chloride and NaOH were added to the extract in different ratios, yielding optimal precipitation in 1:1 ratio with 10 g of extract. Bulk synthesis was conducted, followed by magnetic stirring to observe color change and precipitation. The prepared nanoparticles were applied to dye degradation studies in order to assess the pH, concentration, effects of dosage, and contact time on methylene blue degradation efficiency and kinetic studies.

Results: Adsorption followed pseudo-first-order kinetics, with removal efficiency of 85% at pH 12 and 550 mg l⁻¹ dye concentration, showing a maximum removal efficiency at a contact time of 180 min.

Interpretation: The findings suggest that green-synthesized iron oxide nanoparticles offer a sustainable, cost-effective alternative to conventional adsorbents for wastewater treatment, with the potential for reuse after regeneration.

Key words: Dye degradation, Green-synthesis, Iron oxide nanoparticles, *Lantana camara*, Methylene blue dye



Introduction

The rapid expansion of textile industry has contributed significantly to global economic growth, generating around \$1 trillion annually and accounting for approximately 7% of the world's total exports. However, this growth comes with severe environmental consequences, particularly due to the widespread use of synthetic dyes such as methylene blue, which are chemically stable and difficult to degrade when released into open water resources (Khan *et al.*, 2015). Methylene blue is used therapeutically in clinical settings, particularly for the treatment of methemoglobinemia, in doses less than 2 mg kg⁻¹. However, excessive doses can lead to toxicity, including cardiac arrhythmias, decreased cardiac output, reduced renal and mesenteric blood flow, coronary vasoconstriction, impaired gas exchange, and increased pulmonary vascular pressure and resistance (Feiona *et al.*, 2021). Additionally, it may cause bluish discoloration of skin and mucosa and greenish-blue discoloration of urine, posing a severe threat to aquatic and human health.

Traditional methods of wastewater treatment, such as chemical precipitation and activated carbon adsorption, often fall short in completely removing synthetic dyes from wastewater, leading researchers to explore advanced materials for more efficient dye degradation. Over the past years, there has been increasing interest in the green synthesis of iron oxide nanoparticles using plant extracts. These biogenic nanoparticles combine high surface area, magnetic properties, and low toxicity, making them ideal candidates for environmental remediation. For instance, iron oxide nanoparticles synthesized using *Azadirachta indica* (Akhtar *et al.*, 2024) and *Annona muricata* (Jose *et al.*, 2020) leaf extracts have demonstrated effective methylene blue degradation. Despite this progress, research on the use of *Lantana camara* for nanoparticle synthesis remains scarce, even though its biomass is widely available and rich in bioactive compounds. *Lantana camara*, a globally invasive plant species, has been studied for biochar production in dye removal (Kundu *et al.*, 2024). Still, its potential as a precursor for iron oxide nanoparticles has been largely overlooked.

This is surprising given that *Lantana camara* contains metabolites like triterpenes, flavonoids, and phenylethanoid glycosides (Laha *et al.*, 2022), which can act as natural reducing and stabilizing agents during nanoparticle synthesis. Harnessing this invasive weed for nanoparticle production not only addresses environmental concerns but also transforms a problematic species into a valuable resource for sustainable water treatment. In view of the above, this research was conducted to explore a cost-effective method for methylene blue dye degradation using green-synthesized iron oxide nanoparticles from *Lantana camara* leaf extract. The research focuses on optimizing process parameters, including initial and final dye concentrations, solution pH, adsorbent dosage, and contact time, to maximize degradation efficiency. Furthermore, the study assesses nanoparticle reusability to determine long-term viability, addressing critical gap in sustainable wastewater treatment solutions. This work contributes

to the evolving field of green nanotechnology by demonstrating how an invasive plant species can be repurposed to mitigate industrial pollution, offering an eco-friendly and scalable alternative to traditional dye degradation methods.

Materials and Methods

Nanoparticle synthesis: Fresh leaves of *Lantana camara* were collected from Siruseri (12°50'6.6" N, 80°12'4.2" E), a southern suburb of Chennai, Tamil Nadu, India. Identification of *Lantana camara* was performed based on morphological features and cross-verified with images and descriptions from eFlora. No formal taxonomic verification or voucher specimen was obtained. The collected leaves of *Lantana camara* were washed thoroughly to remove dust. The leaves were oven-dried at 50°C, finely ground into powder, and stored in a glass container. Samples at varying concentrations (1 g, 5 g, 10 g, and 15 g) were dissolved in 100 ml of distilled water and agitated at 200 rpm for 3 hrs. The brown-colored extract was filtered using Whatman No. 40 filter paper, following the procedures outlined by Philip (2010).

Synthesis of iron oxide nanoparticles: Iron oxide nanoparticles (FeONPs) were synthesized using 0.1 M ferric chloride hexahydrate (FeCl₃·6H₂O) as a precursor. The plant extract and precursor were combined in varying ratios (1:1, 1:5, 1:10), and 1 ml of NaOH solution was added. The mixtures were stirred on a magnetic stirrer for 30 min, producing a dark brown solution, signifying the formation of iron oxide nanoparticles (FeONPs). A clear precipitation was observed at 1:1 ratio when 10 g of plant extract was used, which was selected as an optimal concentration for further experiments.

For bulk production, 500 g of the adsorbent was dispersed in 5 l distilled water and agitated at 200 rpm for 3 hrs. The extract was filtered, yielding 3 l of solution, and combined with 3 l of precursor solution. NaOH (50 ml, 0.1 N) was added dropwise while stirring at 50°C, resulting in a color change from brown to black. After 24 hrs of incubation, the precipitate was centrifuged, dried, ground and heated to 300°C for 3 hrs in a muffle furnace to enhance its porosity and magnetic properties. The synthesized nanoparticles were stored for future applications.

Characterization techniques: The surface functional groups of the synthesized iron oxide nanoparticles were investigated using FT-IR spectroscopy (Model: ALPHA II, Bruker, Germany) in the 650–4000 cm⁻¹ range. To study the surface morphology and texture of the nanoparticles, scanning electron microscopy (SEM) (Model: TESCAN OXFORD, Czech Republic) was conducted.

Batch sorption studies: Batch sorption studies were carried out to assess the impact of various parameters on dye degradation using iron oxide nanoparticles (FeONPs). The effect of adsorbent dosage was assessed by adding FeONPs (50–550 mg) to 50 ml dye solution (300 mg l⁻¹) in separate conical flasks, which were stirred at 200 rpm at room temperature. Samples were collected at regular intervals (30–230 min), centrifuged, and analyzed for

absorbance using a colorimeter. Filtration and centrifugation were employed to separate the adsorbent from the solution (Ganguly *et al.*, 2020; Lyu *et al.*, 2018). The effect of pH was investigated by adjusting the pH (2–12) of dye solutions containing 50–550 mg of FeONPs using 1 M NaOH or HCl. The flasks were incubated at 37°C, stirred at 200 rpm, and sampled periodically for absorbance analysis. The effect of dye concentration was studied for initial dye concentrations ranging 50 to 550 mg l⁻¹ at room temperature and pH 12. Samples were collected at regular intervals, centrifuged, and the supernatant's absorbance was measured. The effect of contact time was examined using 50 mg l⁻¹ dye solutions with 250 mg of FeONPs over 30–230 min. The degradation efficiency (%) was calculated by the equation given below:

$$\text{Degradation Efficiency (\%)} = \frac{C_o - C_e}{C_o} \times 100$$

C_o and C_e are the initial concentration and equilibrium concentrations of Methylene Blue in mg l⁻¹

Adsorption Isotherm Studies: Adsorption isotherm studies were performed to investigate the distribution of adsorbate molecules between the liquid and solid phases at equilibrium. Both Langmuir isotherm model (Langmuir, 1918) and Freundlich isotherm models (Freundlich, 1906) were used to describe the relationship between the amount of methylene blue dye adsorbed (q_e) and its equilibrium concentration (C_e).

Langmuir Isotherm: This model assumes monolayer adsorption on a homogeneous surface with a finite number of identical binding sites.

$$\frac{C_e}{q_e} = \frac{1}{Q_o} + \frac{C_e}{Q_o}$$

where, q_e (mg g⁻¹) is the adsorption capacity at equilibrium, C_e (mg l⁻¹) is the equilibrium concentration of the adsorbate, Q_o (mg g⁻¹) is the maximum adsorption capacity of monolayer and bis Langmuir constant. The key characteristics of the Langmuir isotherm are represented by a dimensionless separation factor R_L , which indicates the favorability of the adsorption process.

$$R_L = 1/(1 + bC_o)$$

where, C_o is the initial dye concentration (mg l⁻¹).

Freundlich Isotherm: This model describes adsorption on a heterogeneous surface with varying affinities.

$$\log q_e = \log K_f + \frac{1}{n} \log C_e$$

where, K_f and n are Freundlich constants, indicating adsorption capacity and intensity.

Adsorption kinetics study: The adsorption kinetics of Methylene Blue onto FeONPs was studied by pseudo-first-order

and pseudo-second-order kinetics. The suitability of each model was evaluated by comparing experimental data with the model-predicted values through correlation coefficient (R^2) and the sum of squared errors (SSE). A higher R^2 value indicates a better fit of the model to the experimental data.

Pseudo-First-Order Kinetics: This model assumes that the adsorption occurs on a single site and follows first-order reaction kinetics.

$$\ln(q_e - q_t) = \ln q_e - k_1 t$$

q_e and q_t are the amount of dye adsorbed at equilibrium and at time t (mg g⁻¹), and k_1 (min⁻¹) is the pseudo-first order rate constant.

Pseudo-Second-Order Kinetics: The pseudo-second-order model assumes that adsorption follows a second-order reaction mechanism, with adsorption rate dependent on the square of the number of available adsorption sites.

$$\frac{t}{q_t} = \frac{1}{k_2 q_e^2} + \frac{t}{q_e}$$

k_2 is the pseudo-second order rate constant (g mg⁻¹ min⁻¹).

Chemicals: A working dye solution of 300 mg l⁻¹ was prepared by diluting 90 ml of the stock solution (0.1 g of methylene blue in 100 ml of distilled water) with 210 ml of distilled water. The concentration of methylene blue dye was determined using a UV-Vis spectrophotometer (Model: UV-1700, SHIMADZU, India) at 620 nm wavelength. All the chemicals used in the experiments were of analytical grade and were purchased from Hi Media, India.

Results and Discussion

Iron nanoparticles were successfully synthesized using *Lantana camara* leaf extract as a natural reducing and stabilizing agent. Optimal nanoparticle formation occurred at 1:1 ratio of leaf extract to ferric chloride, indicated by a color change from brown to black on adding NaOH. Similar color transitions during green synthesis of iron nanoparticles have been reported earlier (Kundu *et al.*, 2024; Devi *et al.*, 2019; Shah *et al.*, 2014). The synthesized nanoparticles exhibited strong magnetic properties, which were qualitatively tested using a magnet and subsequently used for further characterization.

Fig. 1 illustrates the relationship between sample concentration and absorbance at 620 nm, showing a linear increase in the absorbance. The linear equation $y = 0.0033x$ indicated that for every 1 mg m l⁻¹ increase in the concentration, the absorbance increased approximately by 0.0033 units. A strong linear relationship between absorbance and concentration was confirmed by a high correlation coefficient ($R^2 = 0.9982$). Fourier Transform Infrared Spectroscopy (FTIR) was conducted at room temperature to confirm the functional groups present in

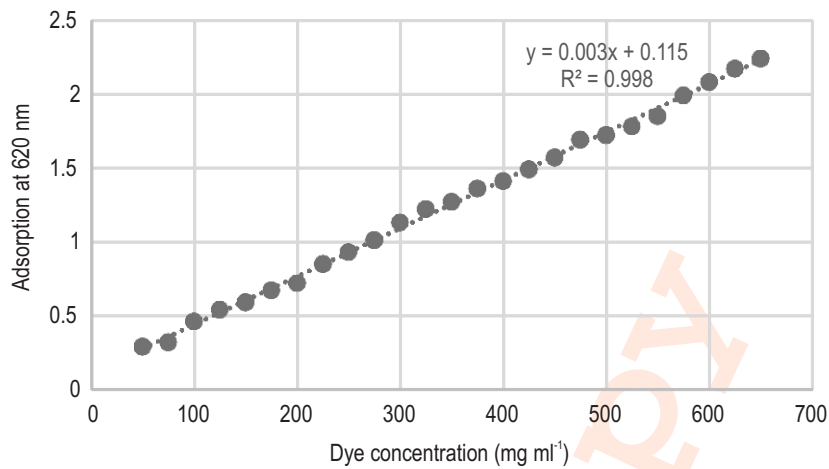


Fig. 1: Standard Curve: Relationship between dye concentration and absorbance at 620 nm.

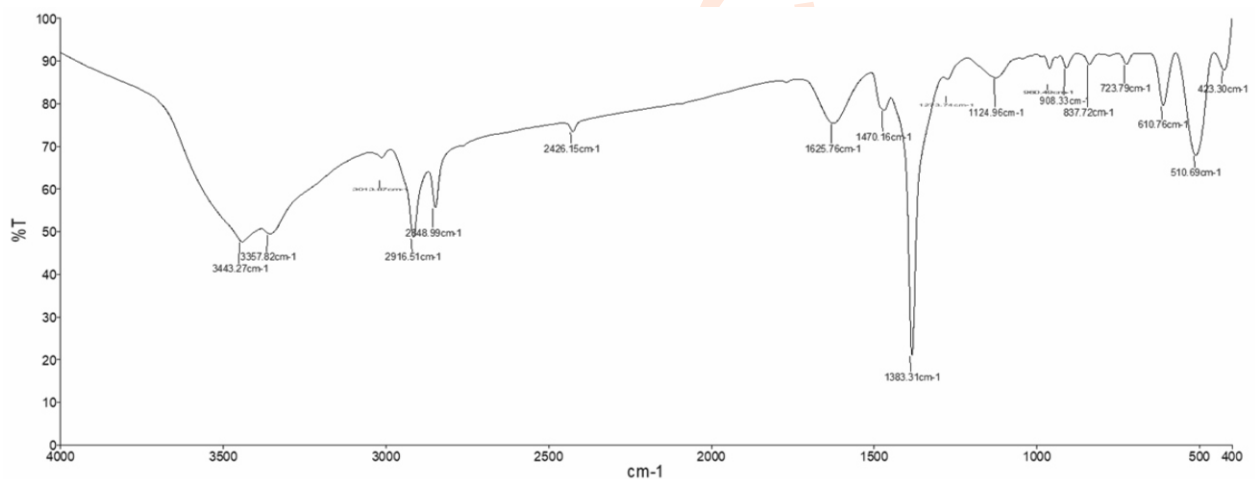


Fig. 2: FTIR spectrum of synthesized iron oxide nanoparticles.

the synthesized iron oxide nanoparticles. The FTIR spectrum (Fig. 2) exhibited well-defined peaks at 510.69 cm^{-1} , 610.76 cm^{-1} , 908.33 cm^{-1} , 1383.31 cm^{-1} , 2648.99 cm^{-1} , 2916.51 cm^{-1} and 3443.27 cm^{-1} . The characteristic Fe-O stretching vibrations at 510.69 cm^{-1} and 610.76 cm^{-1} confirmed the formation of FeNPs synthesized via green deposition method, with 510 cm^{-1} band specifically indicating Fe_3O_4 . These results align with the previous studies, including a 577 cm^{-1} Fe-O peak from *Azadirachta indica* leaf extract (Akhtar *et al.*, 2024), 443 cm^{-1} , 583 cm^{-1} and 634 cm^{-1} Fe-O peaks reported by Sodipo *et al.* (2015) and 663 cm^{-1} , 462 cm^{-1} and 426 cm^{-1} Fe-O peaks from *Platanus orientalis* leaf extract (Devi *et al.*, 2019). These findings confirm the successful synthesis of FeNPs with characteristic Fe-O vibrations, consistent with previously reported green synthesis methods.

The dosage of the adsorbent is a critical factor in degradation studies as it directly affects the adsorption efficiency of iron nanoparticles in removing dyes. Fig. 4A illustrates the impact of varying FeNP dosages on the percentage removal of Methylene blue dye. The removal efficiency increased from 29% to 75% as the dosage of adsorbent increased, indicating an enhanced capacity for adsorption due to increased adsorption sites and surface area. When the adsorbent dosage increased from 50 to 550 mg, the dye removal efficiency significantly improved due to a higher number of adsorption sites available at a constant initial dye concentration, facilitating better dye uptake (Bello and Ahmad, 2011). A key factor defining this behavior is that during adsorption process, active adsorption sites remain unsaturated, even as the number of available sites increase with rising adsorbent dosage (Khattri and Singh, 2009).

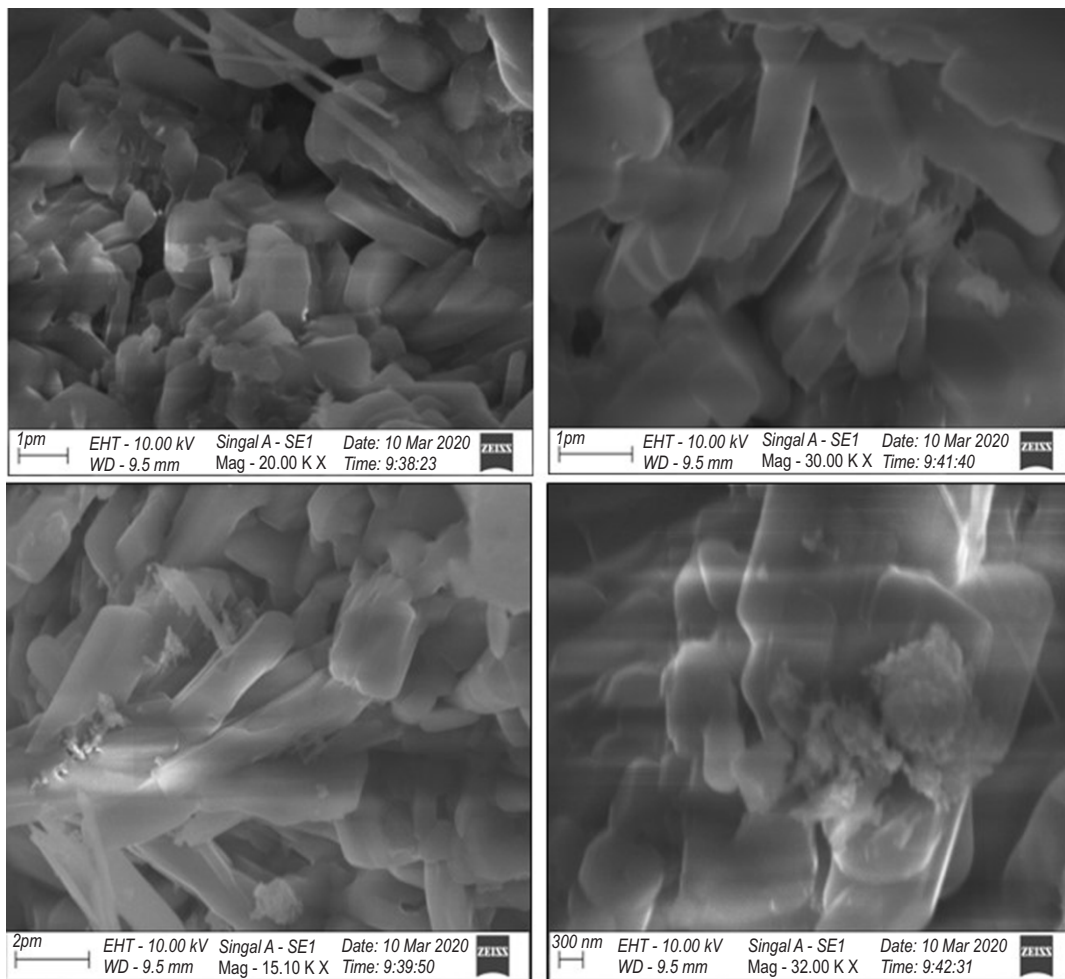


Fig. 3: SEM images of synthesized iron oxide nanoparticles from *Lantana camara* leaf extract.

The interaction between the dye molecules and the adsorbent improved as dye concentration increased. Higher concentrations help to overcome the mass transfer resistance between the solid and aqueous phases (Gautam *et al.*, 2015). A similar trend was noted in the removal of methylene blue dye using biochar derived from the leaves and stems of *Lantana camara* (Kundu *et al.*, 2024). The surface morphology of the synthesized iron oxide nanoparticles (FeONPs) was examined using SEM at various magnifications at 20,000X (Fig. 3a) and 30,000X (Fig. 3b). The SEM micrographs reveal that the FeONPs possess predominantly cuboidal and rod-like shapes (Fig. 3c) with uneven and rough surface textures. The particles appear to be well distributed, but slight agglomeration is evident, particularly in Fig. 3d. This aggregation may be due to the intrinsic magnetic interactions among nanoparticles or the absence of sufficient capping agents, as commonly observed in biosynthesized iron oxide systems (Arokiyaraj *et al.*, 2013). These morphological traits confirm the successful formation of FeONPs with diverse crystalline structures and support their

suitability for surface-based applications such as dye adsorption.

Fig. 4B illustrates that the adsorbed amount of methylene blue increased with rising pH, while adsorption decreased under acidic conditions. The removal efficiency improved from pH 10-12, reaching a maximum efficiency of 85% at pH 12. At low pH, FeONPs showed a positive surface charge, leading to electrostatic repulsion between the cationic methylene blue molecules and the protonated acidic functional groups, such as carboxylates on FeONPs. Additionally, competitive adsorption with H⁺ ions further reduced Methylene blue uptake (Cheera *et al.*, 2017). As a result, adsorption efficiency was significantly lower in acidic conditions. At higher pH levels, FeONPs became negatively charged, promoting strong electrostatic attraction with positively charged Methylene blue molecules. This enhanced interaction leading to greater adsorption efficiency (Mourid *et al.*, 2018). The results confirm that electrostatic attraction and complex formation are the primary mechanisms governing methylene blue adsorption onto

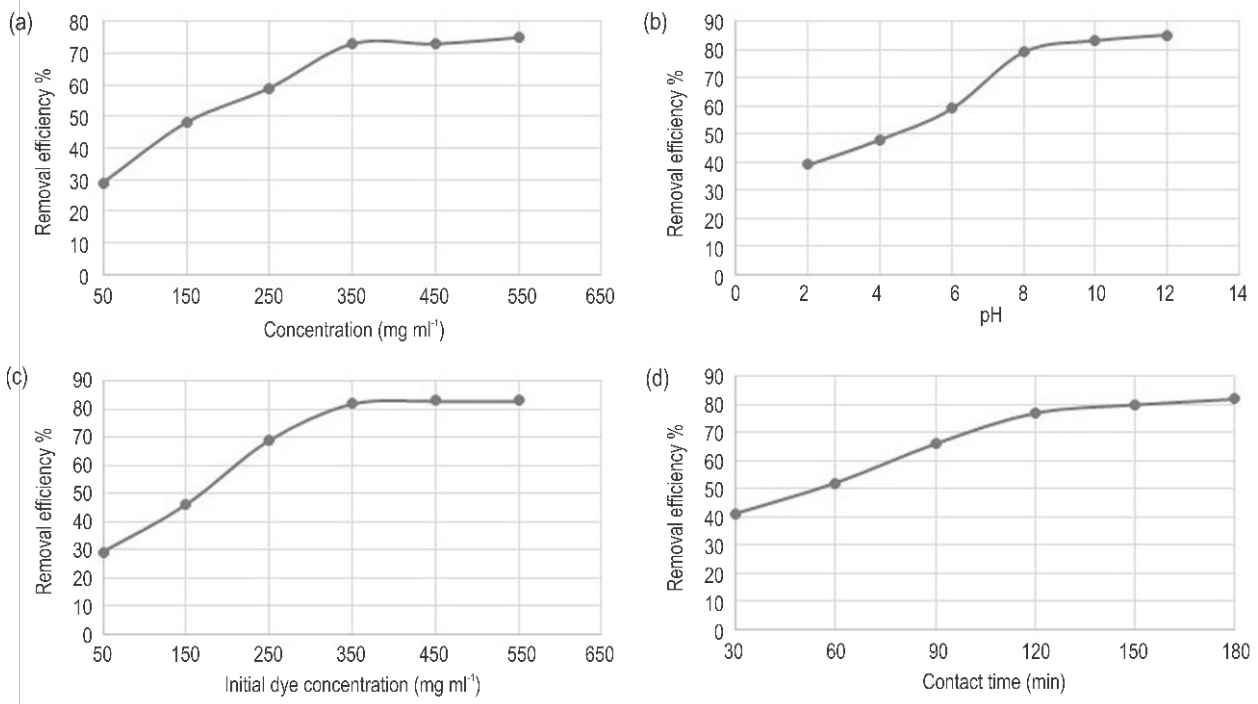


Fig. 4: Effect of adsorption parameters on methylene blue dye removal efficiency: (A) Adsorbent dosage, (B) pH, (C) Initial dye concentration and (D) Contact time.

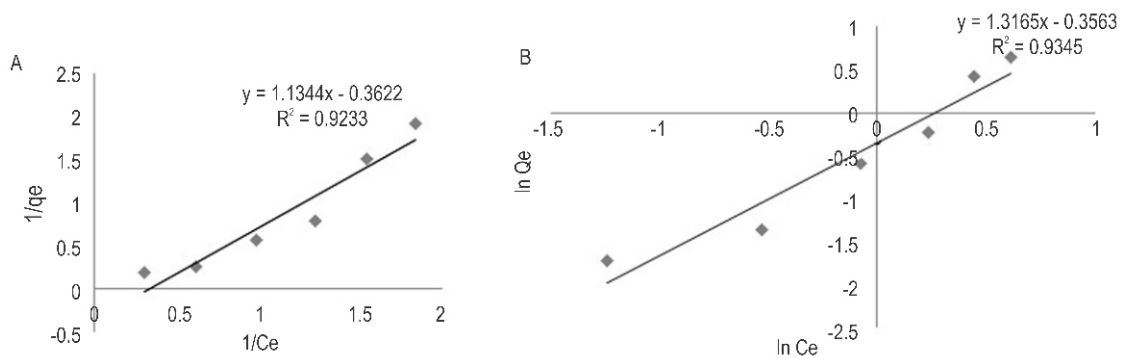


Fig. 5: Adsorption Isotherm Models for methylene blue: (A) Langmuir plot and (B) Freundlich plot.

FeNPs. Similar trends were observed in previous studies, where iron-based adsorbents showed maximum methylene blue adsorption at alkaline pH due to charge interactions (Dermibas *et al.*, 2008; 2009).

The effect of dye concentration on methylene blue degradation efficiency was investigated within a concentration range of 50 to 550 mg l⁻¹ at pH 12 and room temperature. As shown in Fig. 4C, the percentage removal of methylene blue decreased with increasing initial dye concentration, although a

higher dye concentration resulted in a greater absolute amount of degradation. At higher initial concentrations, fewer dye ions competed for active adsorption sites on FeNPs, leading to higher adsorption capacity per unit mass of adsorbent (Idris *et al.*, 2011). The effect of contact time on methylene blue degradation was also examined, revealing that adsorption efficiency increased with time, reaching equilibrium in 120 min (Fig. 4D). A rapid initial adsorption phase occurred within the first 50 min, where more than 40% of the dye was removed across all concentrations. This fast initial degradation can be

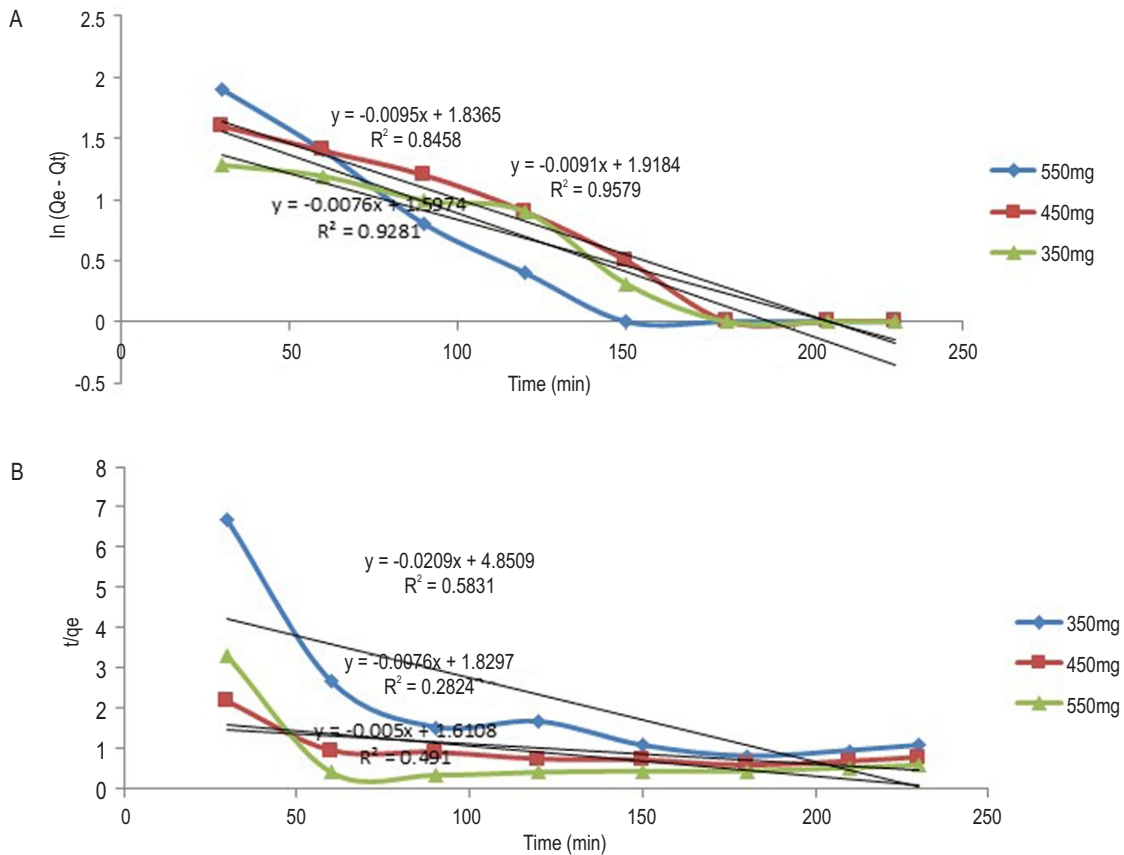


Fig. 6: Comparison of Pseudo-First-Order (A) and Pseudo-Second-Order (B) kinetic models for methylene blue adsorption onto Sorption-Activated *Lantana camara* at different Initial concentrations.

attributed to large number of available active sites on the FeNP surface. However, as adsorption sites became occupied, the rate slowed down due to repulsion between the adsorbed dye molecules and those in solution, leading to equilibrium in an extended time frame (Hwang *et al.*, 2014). These results demonstrate that initial dye concentration and contact time significantly influence MB adsorption efficiency, with optimal adsorption achieved at lower dye concentrations and longer contact times. The adsorption isotherm study revealed that the experimental data fitted both the Langmuir and Freundlich models. The Langmuir isotherm parameters indicated a maximum adsorption capacity (Q^m) of 0.881 mg g^{-1} and a Langmuir constant b of 1.298 Lmg^{-1} and $R^2 = 0.923$, suggesting a favorable monolayer adsorption process (Malik, 2004). Additionally, the dimensionless separation factor R_L was found to be 0.005, confirming high affinity of FeNPs for methylene blue dye. For Freundlich isotherm, the adsorption intensity parameter n was 0.759, and the Freundlich constant (KF) was $3.071 \text{ mg g}^{-1} (\text{Lmg}^{-1})^{1/n}$, indicating heterogeneous surface adsorption. The value of $1/n$ being less than 1 further supports the favorability of adsorption. A comparison of both models suggest that while both can describe the adsorption process, a

slightly higher R^2 value (0.934) for the Freundlich model implies a better fit, indicating that adsorption may involve surface heterogeneity.

The adsorption kinetics of methylene blue onto sorption-activated *Lantana camara* (SALC) were analyzed by pseudo-first-order and pseudo-second-order (PSO) models. The higher R^2 values obtained for pseudo-first-order kinetics at different initial dye concentrations (C_0) 350 mg l^{-1} ($R^2 = 0.845$), 450 mg l^{-1} ($R^2 = 0.957$), and 550 mg l^{-1} ($R^2 = 0.928$) showed that the adsorption process is primarily diffusion-driven and physisorption-controlled rather than chemisorption-dominated (Fig. 6). This aligns with the Freundlich isotherm model, suggesting heterogeneous, multilayer adsorption rather than a uniform monolayer adsorption as described by the Langmuir model. Therefore, the Freundlich isotherm is the best fit for describing the adsorption behavior of Methylene blue onto Sorption-Activated *Lantana camara* in this study. The reusability of iron oxide nanoparticles synthesized using *Lantana camara* leaf extract for methylene blue dye degradation depends on their stability, regeneration efficiency and structural integrity after multiple cycles. These biogenic nanoparticles can be

regenerated through desorption techniques such as washing with ethanol, dilute acids or UV irradiation. Their magnetic properties (if Fe₃O₄) allow easy recovery using an external magnet, minimizing material loss. However, repeated adsorption and desorption experiments may lead to slight agglomeration or surface passivation, potentially reducing catalytic efficiency (Nassar, 2010).

Hence, it can be concluded that *Lantana camara* leaves, like other agricultural waste, can be effectively utilized for dye adsorption. The adsorption process adhered to the Freundlich isotherm model ($R^2 = 0.9345$), indicating heterogeneous and multilayer adsorption. Kinetic analysis revealed that the pseudo-first-order model provided a superior fit (higher R^2 values), suggesting a diffusion-driven, physisorption-controlled process. The adsorption capacity was influenced by factors such as adsorbate concentration, adsorbent dosage, pH, contact time, and stirring speed, achieving a maximum removal efficiency of 85% at 120 min. The results indicate that nanoparticles synthesized from *Lantana camara* leaves offer an efficient and sustainable solution for methylene blue removal. Further optimization of synthesis conditions and functionalization can enhance durability, ensuring effective performance over multiple cycles for wastewater treatment.

Acknowledgment

The authors are thankful for the facilities and infrastructure provided by the Department of Biotechnology, Vivekanandha College of Engineering for Women, Namakkal, Tamil Nadu, India.

Authors' contribution: K. Gilbert Ross Rex: Conceptualization, Methodology, Validation; V. Akshaya, S. Santhiya: Data Curation, Conducted Statistical analysis through SPSS Software; P. Bhuvaneshwari: Writing Original draft, Conducted Statistical analysis through SPSS Software; M. Rajamehala: Writing, Revision and Editing.

Funding: This research was conducted without any financial support or funding from external sources.

Research content: The research content of the manuscript is original and has not been published elsewhere.

Ethical approval: This study did not involve any experiments with animals, humans, or plants requiring ethical approval.

Conflict of interest: The authors declare that there is no conflict of interest.

Data availability: All data generated or analyzed during this study are original and included in this article.

Consent to publish: All authors agree to publish the paper in *Journal of Environmental Biology*.

References

- Akhtar, M. S., S. Fiaz, S. Aslam, S. Chung, A. Ditta, M.A. Irshad, A.M. Al-Mohaimed, R. Iqbal, W.A. Al-onazi, M. Rizwan and Y. Nakashima: Green synthesis of magnetite iron oxide nanoparticles using *Azadirachta indica* leaf extract loaded on reduced graphene oxide and degradation of methylene blue. *Sci. Rep.*, **14**, 18172 (2024).
- Arokiyaraj, S., M. Saravanan, N. K. UdayaPrakash, M. ValanArasu, B. Vijayakumar and S. Vincent: Enhanced antibacterial activity of iron oxide magnetic nanoparticles treated with *Argemone mexicana* L. leaf extract: An *in vitro* study. *Mater. Res. Bull.*, **48**, 3323–3327 (2013).
- Bello, O.S. and M.A. Ahmad: Adsorption removal of a synthetic textile dye using cocoa pod husk. *Toxicol. Environ. Chem.*, **93**, 1298–1308 (2011).
- Cheera, P., K. Sreenivasulu, S. Gangadhara and P. Venkateswarlu: Bio-inspired green synthesis of Ni/Fe₃O₄ magnetic nanoparticles using *Moringa oleifera* leaf extract: A magnetically recoverable catalyst for organic dye degradation in aqueous solution. *J. Alloys Compd.*, **12**, 363 (2017).
- Dermibas, E., N. Dizge, M.T. Sulak and M. Kobya: Adsorption kinetics and equilibrium studies of copper from aqueous solutions using hazelnut shell activated carbon. *Chem. Eng. J.*, **148**, 480–487 (2008).
- Demirbas, A.: Agricultural-based activated carbons for the removal of dyes from aqueous solutions: A review. *J. Hazard. Mater.*, **167**, 1–9 (2009).
- Devi, H.S., M.A. Boda, M.A. Shah, S. Parveen and A.H. Wani: Green synthesis of iron oxide nanoparticles using *Platanus orientalis* leaf extract for antifungal activity. *Green Process. Synth.*, **8**, 38–45 (2019).
- Feiona, T.A., G. Sabeena, M. S. Bagavathy, E. Pushpalaksmi, J. Jenson Samraj and G. Annadurai: Recent advances in the synthesis and characterization of nanoparticles: A green adeptness for photocatalytic and antibacterial activity. *Nat. Environ. Pollut. Technol.*, **20**, 657–663 (2021).
- Freundlich, H. M. F.: Über die adsorption in lösungen. *Zeitschrift für Physikalische Chemie*, **57**, 385–470 (1906).
- Ganguly, P., R. Sarkhel and P. Das: Synthesis of pyrolyzed biochar and its application for dye removal: Batch, kinetic and isotherm with linear and non-linear mathematical analysis. *Surf. Interfaces*, **20**, 100616 (2020).
- Gautam, R. K., P. K. Gautam, S. Banerjee, V. Rawat, S. Soni, S. K. Sharma and M. C. Chattopadhyaya: Removal of tartrazine by activated carbon biosorbents of *Lantana camara*: Kinetics, equilibrium modeling and spectroscopic analysis. *J. Environ. Chem. Eng.*, **3**, 79–88 (2015).
- Hwang, S.W., A. Umar, G.N. Dar, S.H. Kim and R.I. Badran: Synthesis and characterization of iron oxide nanoparticles for phenyl hydrazine sensor applications. *Sensor Lett.*, **12**, 1–5 (2014).
- Idris, M.N., Z.A. Ahmad and M.A. Ahmad: Adsorption equilibrium of malachite green dye onto rubber seed coat-based activated carbon. *Int. J. Basic Appl. Sci.*, **11**, 305–311 (2011).
- Jose, B. and F. Thomas: Photocatalytic degradation of methylene blue using iron oxide nanoparticles synthesized using *Annona muricata* leaf extract. *Int. J. Pharm. Pharm. Sci.*, **12**, 46–51 (2020).
- Khan, T. A., S. A. Chaudhry and I. Ali: Equilibrium uptake, isotherm and kinetic studies of Cd(II) adsorption onto iron oxide activated red mud from aqueous solution. *J. Mol. Liq.*, **202**, 165–175 (2015).
- Khattri, S. D. and M. K. Singh: Removal of malachite green from dye wastewater using neem sawdust by adsorption. *J. Hazard. Mater.*, **167**, 1089–1094 (2009).

- Kundu, D., P. Sharma, S. Bhattacharya, K. Gupta, S. Sengupta and J. Shang: Study of methylene blue dye removal using biochar derived from leaf and stem of *Lantana camara* L. *Carbon Res.*, **3**, 22 (2024).
- Laha, A., S. Sengupta, P. Bhattacharya, J. Mandal, S. Bhattacharyya and K. Bhattacharyya: Recent advances in the bioremediation of arsenic-contaminated soils: A mini review. *World J. Microbiol. Biotechnol.*, **38**, 189 (2022).
- Langmuir, I.: The adsorption of gases on plane surfaces of glass, mica and platinum. *J. Amer. Chem. Soci.*, **40**, 1361–1403 (1918).
- Lyu, H., B. Gao, F. He, A.R. Zimmerman, C. Ding, J. Tang and J.C. Crittenden: Experimental and modeling investigations of ball-milled biochar for the removal of aqueous methylene blue. *Chem. Eng. J.*, **335**, 110–119 (2018).
- Malik, P.K.: Dye removal from wastewater using activated carbon developed from sawdust: Adsorption equilibrium and kinetics. *J. Hazard. Mater.*, **113**, 81-88 (2004).
- Mourid, E. H., M. Lakraimi, S. El Abrid, L. Benaziz, Elkhatabi and M. Berraho: Use of calcined layered double hydroxide [Zn₂-Al-CO₃] for removal of textile dye acid green 1 from wastewater: Kinetic, equilibrium, comparative, and recycling studies. *Turk. J. Chem.*, **42**, 1146–1160 (2018).
- Nassar, N.N.: Rapid removal and recovery of Pb(II) from wastewater by magnetic nanoadsorbents. *J. Hazard. Mater.*, **184**, 538–546 (2010).
- Philip, D.: Green synthesis of gold and silver nanoparticles using *Hibiscus rosa-sinensis*. *Phys. E Low-Dimens. Syst. Nanostruct.*, **42**, 1417–1424 (2010).
- Shah, S., S. Dasgupta, M. Chakraborty, R. Vadakkekara and M. Hajoori: Green synthesis of iron nanoparticles using plant extracts. *Int. J. Biol. Pharm. Res.*, **5**, 549-552 (2014).
- Sodipo, B.K. and A.A. Azlan: Superparamagnetic iron oxide nanoparticles incorporated into silica nanoparticles by inelastic collision via ultrasonic field: Role of colloidal stability. *AIP Conf. Proc.*, **1657**, 100002 (2015).